21, rue d'Artois, F-75008 PARIS
http : //www.cigre.org

CIGRE US National Committee
2018 Grid of the Future Symposium

Modelling and Control of Static Synchronous Compensators (STATCOMs)

R. RYE
Virginia Tech
USA

K. THOMAS, H.-M. CHOU, D. YANG
Dominion Energy
USA

SUMMARY

This paper focuses on the derivation of an average model and a *dq*-frame controller for a transmission-level utility STATCOM in order to verify the device's functionality during operation. The controller consists of three modes of operation including a fixed reactive power control mode, a voltage control mode, and a voltage control mode with a reactive power controller. All three modes of this controller are used to operate a six-pulse, two-level STATCOM. Additionally, this paper discusses the implementation of the Simplex method to aid in the optimization of the controller gains to ensure expected response times. A series of tests are performed on this controller in all three modes and the results are shown for a grid voltage step test in addition to balanced and unbalanced fault tests. The results obtained are as expected and the response times of the STATCOM controller meet those of vendor reports.

KEYWORDS

STATCOM, dq controller, dq reference frame, controller, Simplex method, FACTS, PSCAD/EMTDC.

beccarye@vt.edu

I. INTRODUCTION

Concerns about the current and future states of the environment have prompted government and non-profit agencies to enact regulatory legislation on fossil fuel emissions. In 2015, electricity generation comprised 29% of total U.S. greenhouse gas emissions with 71% of this generation being due to coal combustion sources [1]. As a result, utilities have retired a number of coal power plants and have employed alternative means of power generation such as renewable energy sources (RES). The variability of available on-demand power introduced by RES, coupled with the increase of overall power demand, has resulted in heavily loaded lines which are affecting system stability and reliability, thus prompting utilities to investigate technology which can regulate line voltages and retain system stability to ensure the customer continues to receive the necessary on-demand power.

Flexible ac transmission systems (FACTS) are being employed by utilities to dynamically control power flow and enhance system stability. FACTS, as defined by IEEE, are power electronic-based systems, and other static equipment, which provide control of one or more ac transmission system parameters to enhance controllability and increase power transfer capability [2][3]. Such devices include thyristor-controlled capacitor or reactor banks, static var compensators (SVCs), and static synchronous compensators (STATCOMs), the last of which will be the focus of this paper.

STATCOMs are shunt-connected devices which exchange reactive power with the ac power system to rapidly control the three-phase voltages at the point of common coupling (PCC), thanks to the use of power electronics in the device's switching network [4][5]. When the PCC voltage is greater than the STATCOM's terminal voltage, the STATCOM absorbs reactive power much like a reactor bank. On the other hand, when the PCC voltage is lower than the STATCOM's terminal voltage, then the STATCOM provides reactive power and is seen as a capacitor bank from the perspective of the grid [4][5]. Otherwise, no reactive power is exchanged if the voltages are equal in magnitude.

In electric transmission, these devices improve transmission quality, reliability, and stability in addition to power transfer capability. In distribution systems, they mainly provide voltage regulation support and can also be used to balance the network to compensate for load imbalances [2][3][5]. However, these devices' controllers are black-boxes to utilities as they are bought from manufacturers and contain proprietary information from said manufacturers. As such, it is a necessity to understand these devices to ensure they operate as per the vendor's reports as well as to guarantee the sequence of operation during system contingencies or faults is correct. To do so, a model and controller can be built in a simulation environment, such as PSCAD/EMTDC, in which both the model's and controller's parameters are tunable and one can delve into the control logic to fully comprehend the device's operation.

This paper is organized as follows: section II discusses and derives the average model of a STATCOM. Section III presents the derivation of a basic STATCOM controller in a synchronous reference frame (SRF). Section IV contains the results of some tests to evaluate the performance of the controller and verifies the obtained results through analysis based off of vendor reports and basic STATCOM functionality. Finally, section V is the conclusion and discusses future work to expand this project and to complete the model and its control.

II. AVERAGE MODEL DERIVATION

The switching topology of STATCOMs used in utilities, regardless of if it is transmission- or distribution-level, is often extremely complex. This network utilizes insulated-gate bipolar transistors (IGBTs) which are fully controllable and are capable of fast switching and low on-state losses at high power, thus making them desirable for use in transmission-level devices [4][5]. As a result, this complex topology can be used in transmission-level applications without the need for ac filters, thus reducing the device's physical footprint, unlike the SVC which requires large 5^{th} and 7^{th} harmonic filters, especially at high power.

It is possible to accurately model the switching network, up to the individual switches, to fully comprehend the converter's operation; this is known as the switching model, which is shown in Figures 1 and 2 for an MMC and two-level topology, respectively. However, one of the main disadvantages with this model is the duration of the simulation due to the high frequency switching which is being simulated. As such, an average model of the switching network is developed since it is really only necessary to understand the dynamics of the average values. While a detailed average model can be developed for an MMC to most accurately represent the STATCOM's functionality as done in [6], this process is time-consuming. Additionally, since the main focus of this paper is on the design of the SRF controller, then the average model is derived for the topology shown in Figure 2, where L_m is the leakage reactance of the transformer referred to the low-side of the transformer.

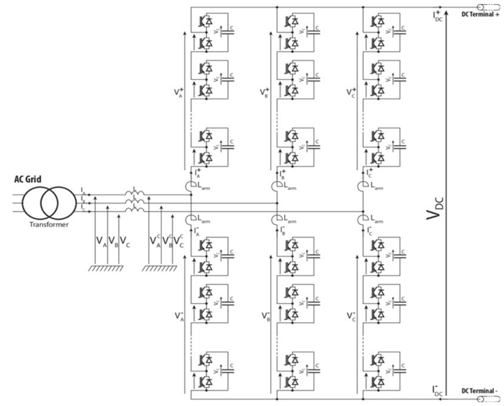

Figure 1: Modular multilevel converter (MMC).

In the voltage source inverter shown in Figure 2, only one switch on each branch can be "on" at any given time. If the positive switch on the *a*-phase branch, S_{ap}, is conducting, then the terminal voltage, v_a, is equal to the dc bus voltage, v_{dc}. Thus, the switching function can be expressed as

$$S_i = S_{ip} = 1 - S_{in}, \quad i \in \{a, b, c\}, \tag{1}$$

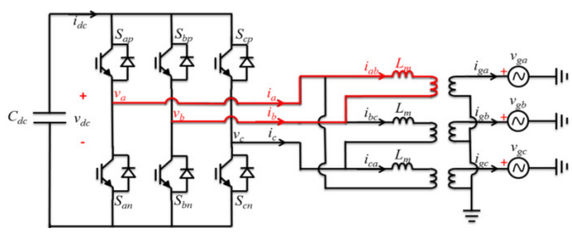

Figure 2: Switching model of 6-pulse, two-level inverter.

and the terminal line voltages of the inverter in Figure 2 can be expressed as

$$v_i = S_i v_{dc}, \quad i \in \{a, b, c\} \tag{2}$$

Additionally, the dc current can be expressed in terms of the three-phase line currents such that when all positive switches are conducting, then the dc current is equal to the sum of the ac currents. For any combination of the switching, the dc current is related to the ac line currents as

$$i_{dc} = S_a i_a + S_b i_b + S_c i_c. \tag{3}$$

Next, Kirchhoff's Voltage Law (KVL) can be used to perform circuit analysis on the lines highlighted in red in Figure 2. However, before doing so, it is important to note that the STATCOM is tied to the grid via a wye-delta transformer, where the converter is on the delta-configured side. Additionally, the measurements which will be used for the control, discussed in section III, are taken on the high-, or wye-configured-, side of the transformer. As such, all grid-side values will be referred to the converter-side of the transformer via the following relationships:

$$v_{gij} = \frac{1}{a} * v_{gi}, \quad i \in \{a, b, c\} \text{ and j} \in \{b, c, a\} \tag{4}$$

$$i_{ij} = a * i_{gi}, \quad i \in \{a, b, c\} \text{ and j} \in \{b, c, a\} \tag{5}$$

where *n* is the turns ratio of the transformer, derived as

$$a = \frac{\frac{rated\ voltage\ on\ wye}{\sqrt{3}}}{rated\ voltage\ on\ delta}. \tag{6}$$

The resulting KVL equation, after substituting in the relationship mentioned in (2) and referring values to the converter side of the transformer via (4) – (6) yields

$$-S_{ab}v_{dc} + L_m \frac{di_{ab}}{dt} + v_{ab} = -S_{ab}v_{dc} + aL_m \frac{di_{ga}}{dt} + \frac{v_{ga}}{a} = 0. \tag{7}$$

As mentioned previously, the average values will be used to develop the control for this device. Applying the averaging function, rearranging variables, and extending to the three phases [5][7], the following is obtained

$$aL_m \frac{d}{dt}\begin{bmatrix}\bar{\imath}_{ga}\\ \bar{\imath}_{gb}\\ \bar{\imath}_{gc}\end{bmatrix} = \begin{bmatrix}d_{ab}\\ d_{bc}\\ d_{ca}\end{bmatrix}\bar{v}_{dc} - \frac{1}{a}\begin{bmatrix}\bar{v}_{ga}\\ \bar{v}_{gb}\\ \bar{v}_{gc}\end{bmatrix} \tag{8}$$

$$\bar{\imath}_{dc} = d_{ab}\bar{\imath}_{ab} + d_{bc}\bar{\imath}_{bc} + d_{ca}\bar{\imath}_{ca}. \tag{9}$$

The final average model is derived from (8) and (9) and is shown in Figure 3.

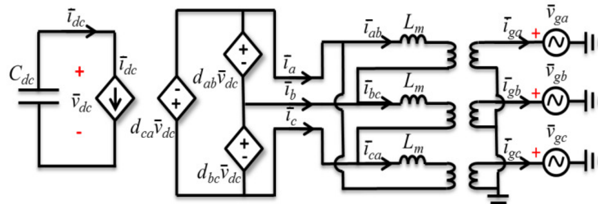

Figure 3: Average model of 6-pulse, two-level inverter.

III. *DQ*-FRAME CONTROLLER

The next step is to develop the controller for the STATCOM's average model discussed in section II. The general controller will consist of three main components in a cascaded control scheme. From the bottom-up, the controller will consist of: (1) an inner loop which provides the modulation signals to the averaged switching network, (2) an outer loop which controls the active power exchange between the STATCOM and grid to regulate the dc bus voltage of the STATCOM, and (3) another outer loop which controls the reactive power exchange between the STATCOM and grid.

In order to simplify the control scheme for the STATCOM and enable the use of a simple proportional-integral (PI) compensator, the three ac quantities from (8) and (9) will be converted to two dc quantities by performing the transformation from the stationary *abc* reference frame to the rotating *dq* SRF via the Park transform [8]. By performing this action, one can use classical control design methods to design a controller.

To begin the design of the controller, (7) is transformed to the rotating *dq*-frame via (10) to obtain (11).

$$\begin{bmatrix}d\\ q\\ 0\end{bmatrix} = \frac{2}{3}\begin{bmatrix}\cos(\theta) & \cos\left(\theta - \frac{2\pi}{3}\right) & \cos\left(\theta + \frac{2\pi}{3}\right)\\ \sin(\theta) & \sin\left(\theta - \frac{2\pi}{3}\right) & \sin\left(\theta + \frac{2\pi}{3}\right)\\ 0.5 & 0.5 & 0.5\end{bmatrix}\begin{bmatrix}a\\ b\\ c\end{bmatrix} \tag{10}$$

$$aL\frac{d}{dt}\begin{bmatrix}\bar{\imath}_d\\ \bar{\imath}_q\\ \bar{\imath}_0\end{bmatrix} = \begin{bmatrix}d_d\\ d_q\\ d_0\end{bmatrix}\bar{v}_{dc} - \frac{1}{n}\begin{bmatrix}\bar{v}_{gd}\\ \bar{v}_{gq}\\ \bar{v}_{g0}\end{bmatrix} - aL\begin{bmatrix}0 & -\omega & 0\\ \omega & 0 & 0\\ 0 & 0 & 0\end{bmatrix}\begin{bmatrix}\bar{\imath}_d\\ \bar{\imath}_q\\ \bar{\imath}_0\end{bmatrix} \tag{11}$$

The last term in (11) is a result of the coupling between the two channels. Since in dc, inductors become short-circuits, it is important to retain the voltage drop across these passive components to ensure the mathematical model matches the physical model, regardless of the reference frame. Rearranging (11) and taking into account that the inner loop's purpose is to drive the current error to zero, then

$$\begin{bmatrix}d_d\\ d_q\end{bmatrix} = \begin{bmatrix}(\bar{\imath}_d^* - \bar{\imath}_d)(G_{ci})\\ (\bar{\imath}_q^* - \bar{\imath}_q)(G_{ci})\end{bmatrix} + \frac{L_m}{\bar{v}_{dc}}\begin{bmatrix}0 & -\omega\\ \omega & 0\end{bmatrix}\begin{bmatrix}\bar{\imath}_d\\ \bar{\imath}_q\end{bmatrix} + \frac{1}{\bar{v}_{dc}}\begin{bmatrix}\bar{v}_{gd}\\ \bar{v}_{gq}\end{bmatrix}. \tag{12}$$

where reference values are indicated with an asterisk. The term on the left-hand side of (12) is the control input; in the case of the STATCOM average model, this is the duty cycle. The first term on the right-hand side of (12) is the output of the PI. The second term represents the decoupling of the two channels in the *dq* frame and the last term consists of the disturbance input, in this case the grid. This equation forms the basis of the innermost loop: the current loop. In this loop, the error of the measured current at the PCC and the reference current, which will be discussed next, is the input of the PI compensator and the output is the control signal, or the duty cycle. Thus, the loop gains of this innermost loop for both the *d*- and *q*- channels are

$$d_d = \frac{(i_d^* - i_d)\left(k_{pi} + \frac{k_{ii}}{s}\right) + v_{gd} - \omega L i_q}{v_{dc}} \tag{13}$$

and

$$d_q = \frac{(i_q^* - i_q)\left(k_{pi} + \frac{k_{ii}}{s}\right) + v_{gq} + \omega L i_d}{v_{dc}}, \tag{14}$$

where k_{pi} and k_{ii} are the gains of the PI compensators in the inner current loop.

As mentioned in the beginning of this section, there are two outer loops. First, it is important to note that the active and reactive powers, respectively in the *dq*-frame are derived as [5][7]

$$P = 1.5 * (v_d i_d + v_q i_q) \tag{15}$$

$$Q = 1.5 * \left(v_q i_d - v_d i_q\right). \tag{16}$$

By convention, v_q is set to 0 due to the nature of the transformation to the synchronous reference frame, thus the active power can be directly controlled by the *d*-channel current and the reactive power can be directly controlled by the *q*-channel current since the two channels are decoupled.

The first outer loop is used to (1) regulate the dc bus voltage of the STATCOM through the exchange of active power, *P*, with the grid and (2) provide the *d*-channel current reference, i_d*, to the inner loop. Since the *d*-channel current can be used to directly regulate this active power exchange, then the deviation of the dc bus voltage from its nominal value can be compensated by also using a PI compensator to obtain

$$i_d^* = (v_{dc}^* - v_{dc})\left(k_{pdc} + \frac{k_{idc}}{s}\right) \tag{17}$$

where k_{pdc} and k_{idc} are the gains of the PI compensator in the dc voltage loop.

The second outer loop is more complex as the STATCOM has three modes of operation. The first mode is known as fixed reactive power mode (FQM) in which the STATCOM provides a set amount of reactive power per a set point determined by an operator. In this mode, the STATCOM operates much like a fixed capacitor or reactor bank. The second mode is known as voltage control mode (VCM) in which the STATCOM dynamically adjusts the reactive power absorption or injection according to the deviation of the PCC voltage to a reference value set by an operator, similar to a synchronous condenser. The last mode is known as voltage control mode with reactive power control (VCM + Q). In this mode, the STATCOM will also provide a fixed amount of reactive power per a reactive power reference, *Q**, set by the operator; however, if the PCC voltage is measured to exceed limits set by the operator, for example ±0.05 pu, then the STATCOM will switch to operate in purely VCM to regulate the voltage back to within the bandwidth set by the utility. Regardless of the mode of operation, this outer loop will provide the inner current loop with a reactive current reference, i_q*, to exchange reactive power with the grid. Thus, the *q*-channel current reference in FQM, specifically, is

$$i_q^* = (Q^* - Q)\left(k_{pq} + \frac{k_{iq}}{s}\right) \tag{18}$$

where k_{pq} and k_{iq} are the gains of the PI compensator in the FQM loop. For VCM, the gains will be k_{pvcm} and k_{ivcm} and for VCM + Q, the gains will be the product of the VCM gains with the Q-controller gains k_{pvcmQ} and k_{ivcmQ} in the VCM loop. Figure 4 depicts the physical system, in black, coupled with the general control layout, in blue. Figure 5 shows how the VCM controller, in blue, works with the Q-controller, in red.

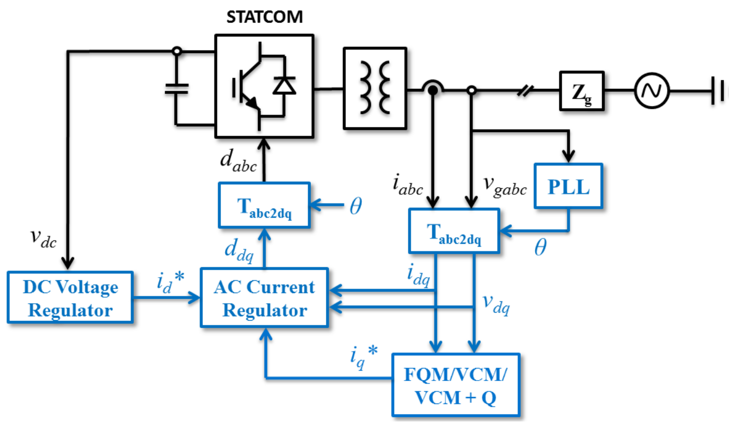

Figure 4: General control scheme for a grid-tied STATCOM.

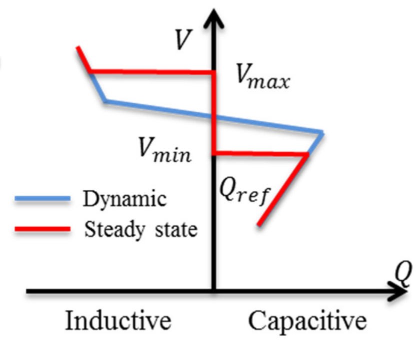

Figure 5: VQ characteristics of a STATCOM.

The last step in developing the dq-frame controller is to tune the PI compensators to ensure the loops do not interact with one another. The innermost loop should be designed to be the fastest so as to quickly react and alter the duty cycles of the STATCOM's averaged switching network when there is a system event or contingency. In order to tune the innermost loop's PIs, a static reference should be provided. Since the STATCOM should ideally not exchange active power with the grid, then i_d* is set to zero. Likewise, i_q* should be set to provide the equivalent reactive power desired. Once these references are provided, the PI gains are initially tuned using a non-linear optimization algorithm, specifically the Simplex method of Nelder and Mead [9]. This method evaluates the objective function at each of the vertices of a starting simplex, where a simplex is some geometric object formed by N+1 points in the N-dimensional space. The vertex with the highest objective function is discarded and replaced with a new vertex. This process repeats until an optimal point is obtained. In this case, the simplex has two dimensions with three points, since there are two gains which are being tuned for each PI. A more in-depth example is discussed in [9]. However, care should be taken to ensure that the initial gain values used to determine the first set of vertices are chosen keeping in mind the specific control loop's function. For example, while the inner loop gains are large and positive, the dc loop will have smaller, negative gains. Additionally, it should be noted that this method does not necessarily optimize the gains and some additional fine-tuning must be done after the iterative process in order to obtain sensible response times or response times which match that of the physical device for each mode of operation.

Once the PI gains for the innermost loop are obtained, then the FQM or VCM gains can be tuned via the same iterative and fine-tuning method. Since these loops only provide i_q*, then i_d* can be maintained at a value of zero. It should be ensured that the outer loops are around ten times slower than the inner loop so as to prevent interaction between the two loops. With the gains of these two loops optimized, then the dc voltage loop can be tuned. Again, this loop should be slower than the innermost loop. Lastly, the Q-controller in the VCM loop should be tuned to be slower than VCM since the main purpose of VCM is to rapidly react to system changes while the Q-controller slowly regulates the reactive power exchange to the operator's set point.

IV. RESULTS

The developed controller underwent a series of tests for each mode of operation. In FQM, the STATCOM controller does not consider the PCC voltage. As such, regardless of any change in voltage magnitude at the PCC, the STATCOM will provide the reactive power as set by the operator,

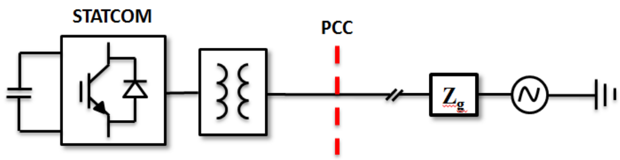

Figure 6: Simulation testbed.

similar to a fixed reactor or capacitor bank. Since this mode of operation is not affected by system dynamics – other than to block or trip, in which the functionality is not included in the controller – then the only results discussed in this section are those due to the operation of the STATCOM under VCM or VCM + Q. The testbed for these simulations is shown in Figure 6.

The first test steps the grid voltage from 1 pu to 0.9652 pu at *t1* while the STATCOM operates in VCM, in which the results are shown in Figure 7. As can be seen, the voltage at the PCC remains relatively unchanged despite the significant grid voltage change thanks to the reactive power injection when the grid voltage steps. Additionally, the reactive current, i_q, closely tracks its reference, i_q*, as desired. This is an indication that the STATCOM controller is working as expected and that the controller does not oscillate and result in unsatisfactory nor unwanted performance, respectively. Lastly, the response time to the grid voltage step is very fast, as expected, since the STATCOM is operating in VCM.

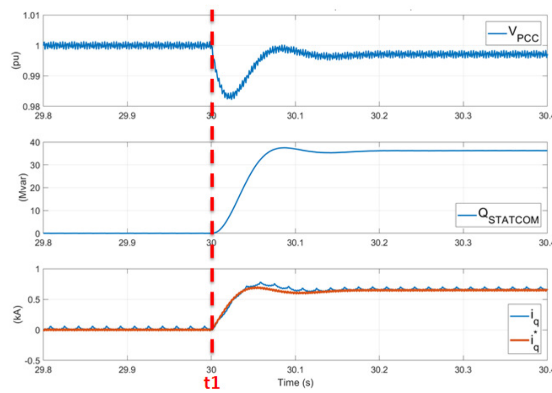

Figure 7: q-channel results of grid step test under VCM.

The same step test is performed when the STATCOM operates in VCM + Q. Figure 8a shows the results from the reactive power controller while Figure 8b zooms in on the dynamic response from the VCM. Compared to the STATCOM under VCM, the response of the device is such that the STATCOM quickly responds to the voltage step change by injecting reactive power almost immediately in an attempt to bring the PCC voltage back to a set reference. However, the STATCOM then slowly regulates the reactive power exchange with the grid to the reactive power reference set by the operator; in this case, 25 Mvar. As expected, the STATCOM does not regulate the PCC voltage since the measured voltage magnitude is within the bandwidth set by the operator; in this case, the region in which the reactive power controller is active is set to be between 0.95 and 1.05 pu. As can be seen, the reactive current closely follows the reactive current reference, which is provided by the VCM + Q loop, thus indicating a successful controller operation.

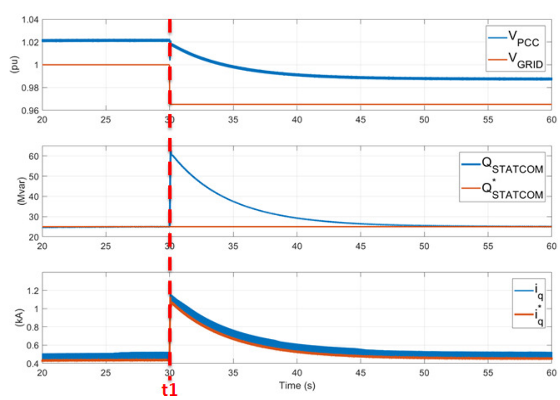

Figure 8a: q-channel results of grid step test under VCM + Q.

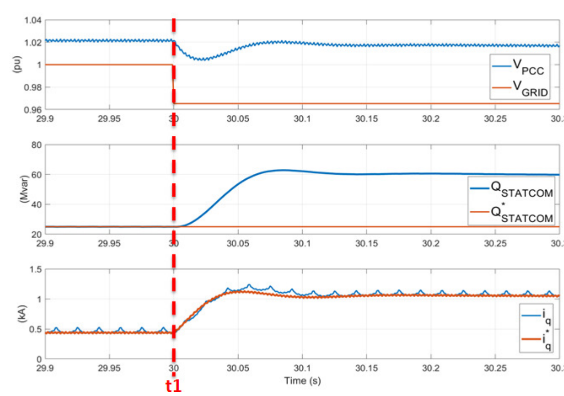

Figure 8b: Zoomed in to show dynamics due to VCM.

The next set of tests performed were fault tests. Figure 9 shows the STATCOM's response to a single line-to-ground fault while in VCM. At $t = 5$ *s*, the fault begins and is cleared after 0.75 seconds. As expected, when the PCC voltage dips, the STATCOM quickly responds by injecting reactive power into the grid to bring the voltage back to around the reference point set by the operator, in this case 1 pu. Likewise, when the fault is cleared, the STATCOM quickly regulates the reactive power exchange with the grid to zero since there is no event causing the voltage at the PCC to deviate enough from the reference point to warrant a considerable reactive power exchange with the grid. It should be noted that the oscillation present in Figure 9 is due to the negative sequence present during an unbalanced fault. Since the *dq* SRF rotates in the *abc* direction at the line frequency, in this case 60 Hz, while the negative sequence rotates in the *acb* direction at the same line frequency with respect to the stationary reference frame, then from the perspective of the *dq*-frame, this is a 120 Hz oscillation.

In a balanced fault, where the three phases connect with the same ground, as shown in Figure 10, there is no 120 Hz oscillation since there is no negative sequence component. Regardless, the STATCOM responds in the same dynamic manner. It should also be noted that the reactive power required to maintain the PCC voltage at the reference value in the case of a balanced fault is significantly greater than the reactive power required to maintain the PCC voltage at the same reference value in the case of a single-phase unbalanced fault. This is expected.

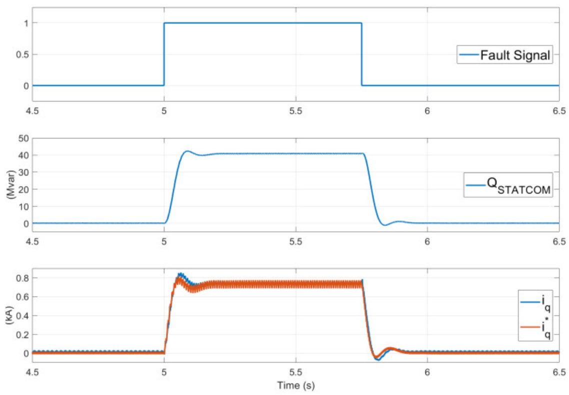

Figure 9: A-G fault test under VCM.

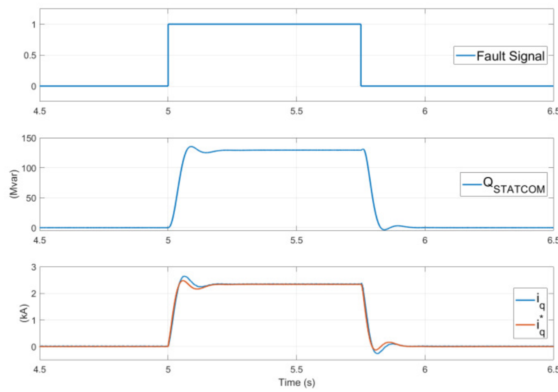

Figure 10: ABC-G fault test under VCM.

V. CONCLUSION & FUTURE WORK

In conclusion, an average model for a six-pulse, two-level, transmission-level STATCOM is derived and used to develop a generic control scheme for this device. The controller includes three primary modes of operation including a fixed reactive power control mode, a voltage control mode, and a voltage control mode with a reactive power control component. The controllers are first tuned by optimizing the controller gains by using the Simplex method in PSCAD/EMTDC and then fine-tuned in order to match the response time of the STATOM model to that of the physical model. The results of a voltage step test in two of the three modes of operation are shown as well as the STATCOM's response to unbalanced and balanced faults. The preliminary results show that the controller operates as expected and according to vendor reports thus far.

In the future, the controller should be expanded to incorporate advanced functionality, such as gain changes, which are a function of system strength, and negative sequence control, to name a few. Additionally, the results of the model built in PSCAD/EMTDC should be compared with that of the vendor's model in the same simulation environment. The derived model and controller operation should also be compared to that of a real controller, either via hardware-in-the-loop (HIL) or using digital fault recorder (DFR) data as the model's system disturbance input. The latter option should also be used for performance evaluation of physical STATCOMs in the power system. Lastly, interaction studies can be performed in a simulation environment which also utilizes HIL to investigate system stability of multiple FACTS devices in electrically close proximity.

BIBLIOGRAPHY

[1] United States Environmental Protection Agency, "Inventory of U.S. Greenhouse Gas Emissions and Sinks: 1990-2015," p. 104, 2017.

[2] "Proposed terms and definitions for flexible AC transmission system (FACTS)," in IEEE Transactions on Power Delivery, vol. 12, no. 4, pp. 1848-1853, Oct 1997.

[3] A. K. Sahoo, K. Murugesan and T. Thygarajan, "Modeling and simulation of 48-pulse VSC based STATCOM using simulink's power system blockset," 2006 India International Conference on Power Electronics, Chennai, 2006, pp. 303-308.

[4] B. Singh, R. Saha, A. Chandra and K. Al-Haddad, "Static synchronous compensators (STATCOM): a review," in IET Power Electronics, vol. 2, no. 4, pp. 297-324, July 2009.

[5] A. Yazdani, R. Iravani, *Voltage-Sourced Converters in Power Systems: Modeling, Control, and Applications*. Hoboken, NJ: John Wiley & Sons, Inc., 2010.

[6] H. Yang, Y. Dong, W. Li and X. He, "Average-Value Model of Modular Multilevel Converters Considering Capacitor Voltage Ripple," in IEEE Transactions on Power Delivery, vol. 32, no. 2, pp. 723-732, April 2017.

[7] F. Shahnia, S. Rajakaruna, A. Ghosh, *Static Compensators (STATCOMs) in Power Systems*. New York: Springer, 2015

[8] S. Hiti, "Modeling and Control of Three-Phase PWM Converters," Ph.D. Dissertation, College of Eng., Virginia Tech, Blacksburg, Virginia, 1995.

[9] A. M. Gole, S. Filizadeh, R. W. Menzies and P. L. Wilson, "Optimization-enabled electromagnetic transient simulation," in IEEE Transactions on Power Delivery, vol. 20, no. 1, pp. 512-518, Jan. 2005.